

Supporting Information

Enhanced electrochemical oxygen and hydrogen evolution reactions using NU-1000@NiMn-LDHS composite electrode in alkaline electrolyte

Soheila Sanati, Reza Abazari, Ali Morsali*

Department of Chemistry, Tarbiat Modares University, P.O. Box 14115-175, Tehran, Iran

*E-mail: morsali_a@modares.ac.ir

Materials. All compounds and solvents: (4-(methoxycarbonyl)phenyl)boronic acid (Merck, 98%), 1,3,6,8-Tetrabromopyrene (Aldrich, 97%), tetrakis(triphenylphosphine) palladium(0) (Strem Chemicals, 99%), $ZrCl_4$ (Aldrich, 99.5%), nickel(II) nitrate hexahydrate ($Ni(NO_3)_2 \cdot 6H_2O$, Merck, 98%), manganese(II)acetate tetrahydrate ($Mn(COOH)_2 \cdot 4H_2O$, Merck, 99%), hexamethylenetetramine (HMTA, Merck, 99%), K_3PO_4 (Aldrich), benzoic acid (Aldrich, 99.5%), ethanol (EtOH), methanol (MeOH), hydrochloric acid (HCl, Aldrich, 37%) and N,Ndimethylformamide (DMF, Merck) were analytical grade and used without further purification.

Synthesis of 1,3,6,8-tetrakis(*p*-benzoic acid)pyrene 1,3,6,8-tetrakis(*p*benzoic acid)pyrene (TBAPy). NU-1000 was synthesized in compliance with the reported processes.^{S1} Typically, a mixture of 1,3,6,8-tetrabromopyrene (0.500 g; 0.97 mmol), (4-(methoxycarbonyl)phenyl)boronic acid (1.040 g; 5.80 mmol), potassium tribasic phosphate (1.100 g; 5.30 mmol), and tetrakis (triphenylphosphine) palladium(0) (0.030 g; 0.026 mmol) was loaded and capped in dry dioxane (20 mL) (in a glovebox) into a 20 mL microwave vial (Biotage). Next, the mixture was shaken in an oil bath at 130 °C for 72 hours under argon atmosphere. Then, the reaction mixture was dried and washed with water to remove the solid residue and inorganic salt. Moreover, chloroform (three times by 50 mL) was utilized to extract the insoluble substance, and the extract was dried on the magnesium sulfate. Then, the solvent volume reduction under vacuum was observed. Finally, this residue was boiled in tetrahydrofuran for two hours followed by filtration. The resultant filtrate consisted lots of impurities. The process provided 0.58 g of 1,3,6,8-tetrakis(4-(methoxycarbonyl)phenyl)pyrene (82% yield).

In the next stage, the solution consisting of 1.5 g (37.5 mmol) NaOH in 100 mL THF/water (ratio 1:1) mixture was added to a 250-mL round bottom flask containing 0.58 g (0.78 mmol) solid 1,3,6,8-tetrakis(4-(methoxycarbonyl)phenyl)pyrene. The resultant suspension was strongly shaken under reflux overnight. Then, the solvents and water were added under vacuum to form a transparent yellow solution. Afterward, the clear yellow solution was shaken at room temperature for two hours, its pH-value was set at 1 using the concentrated HCl. The resulting yellow solid was filtered and washed with water several times. Then, the crude product was recrystallized from DMF and filtered. Finally, chloroform was applied to wash the product followed by vacuum drying resulting in 0.49 g (91%) pure product H₄TBAPy (Scheme S1).

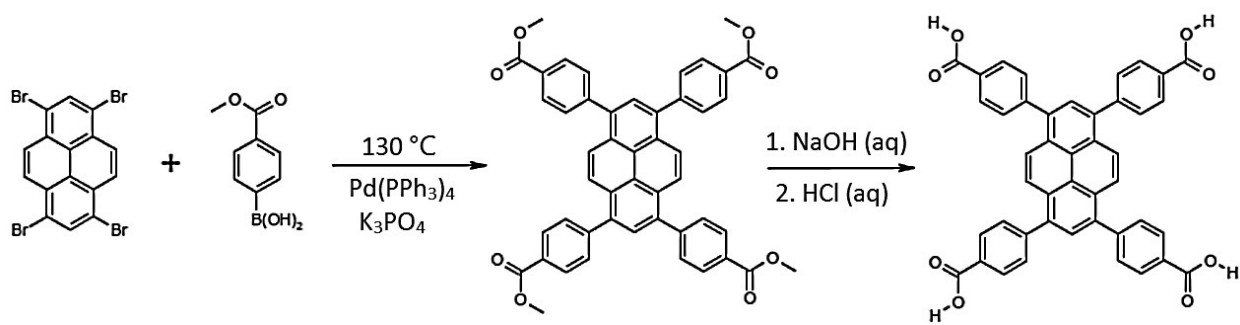
Synthesis of Zr₆(μ₃-OH)₈(OH)₈(TBAPy)₂ (NU-1000). According to the research design, 2700 mg (22 mmol) of benzoic acid and 70 mg of ZrCl₄ (0.30 mmol) were blended in 8 mL of DMF (in a 6-dram vial) and treated by ultrasonication to dissolve. In the next stage, an oven was used to incubate the transparent solution at 80 °C for one hour. Upon cooling to room temperature, 40 mg (0.06 mmol) of H₄TBAPy was poured into the solution and the sonication was continued for 20 min. An oven was used to heat the yellow suspension at 120 °C for 48 hours. Again, upon cooling of the suspension to room temperature, the filtration process (35 mg of the actuated substance with a 54% yield) was chosen to isolate the yellow poly-crystalline substance. Then, DMF was used to wash the product which was consequently actuated with HCl as reported in Feng et al.'s study.^{S2}

Preparation of NU@LDHS composites. In this stage, a one-step solvothermal procedure was applied to prepare NU@LDHS composites. A given content of the as-prepared NU-1000 powder was distributed in DI water (40 mL) and mixed through ultrasonication. Afterward, Ni(NO₃)₂·6H₂O (60 × 10⁻³ M), Mn(COOH)₂·4H₂O (20 × 10⁻³ M), and HMTA (1.12 g) were

poured into the mixture followed by shaking at room temperature for 20 min. The suspension was then transported into a 60-mL Teflon-lined stainless steel autoclave and kept it at 80 °C for 15 hours. Upon the cooling of the mixture to room temperature, ethanol and distilled water were used to wash the final solid products for several times. They were then dried at 60 °C. Subsequently, LDH was dispersed in DI water (40 mL) under magnetic stirring for 30 min, Na₂S·9H₂O (50 × 10⁻³ M) was then added and the mixture was stirred for 30 min. The above solution was then transferred to a Teflon-lined autoclave for hydrothermal treatment at 160 °C for 9 h. To compare the results, a pure LDHS was also synthesized using a similar solvothermal procedure without adding NU-1000.

Electrochemical Characterization. According to the research design, all the electrochemical studies were conducted using an Orgiaflex device in the alkaline electrolyte 2.0 M KOH. Therefore, each electrochemical examination was carried out on a standard 3-electrode cell, in which Ag/AgCl, graphite rod, and the fabricated electrode (on Ni foam with the area of 1 * 1 cm²) served as the reference, counter, and working electrodes, respectively. Moreover, the electrochemical impedance spectroscopy (EIS) and linear sweep voltammetry (LSV) (at a scanning rate of 2 mVs⁻¹) were employed to examine the electrocatalytic activities in a frequency range of 100 kHz-100 mHz. Afterward, Z-view software was used to fit the impedance outputs. Moreover, the multistep chronopotentiometry, as well as chronopotentiometry, was exploited to study the electrocatalytic behavior of the samples. Noteworthy, all the potentials of the present research were converted into the RHE potential using the following formula.

$$E_{RHE} = E_{Ag/AgCl} + 0.059pH + E_{Ag/AgCl}^0$$



Scheme S1. Synthetic scheme for H₄TBAPy.

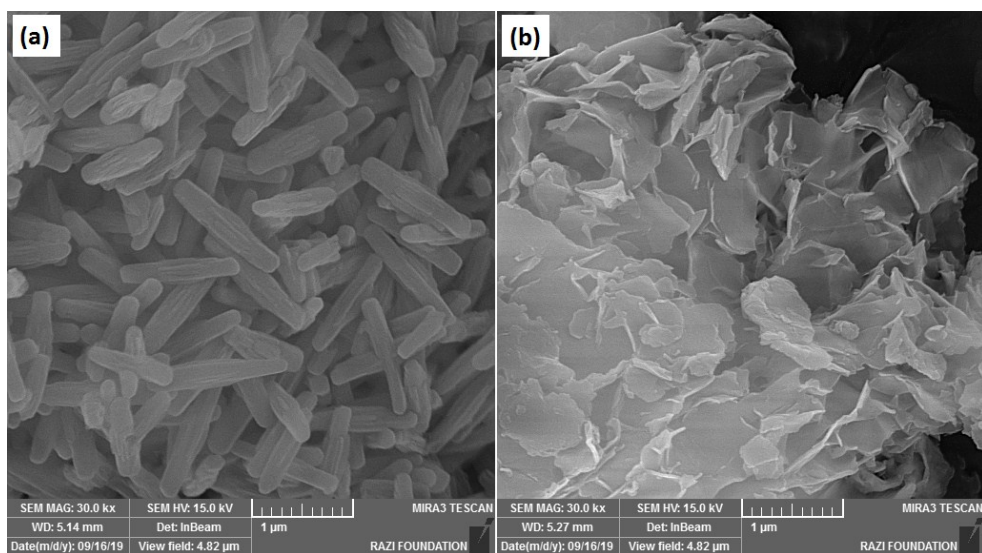


Figure S1. The FE-SEM images of NU (a) and LDHS (b).

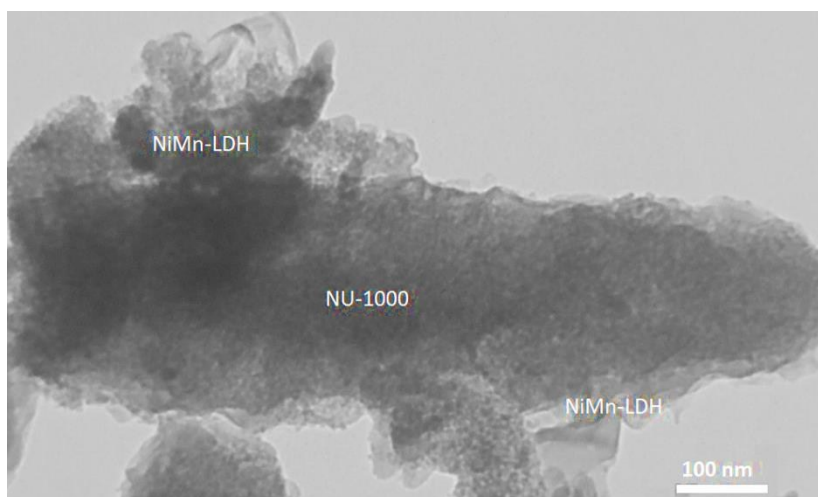


Figure S2. The TEM image of NU@LDHS composites.

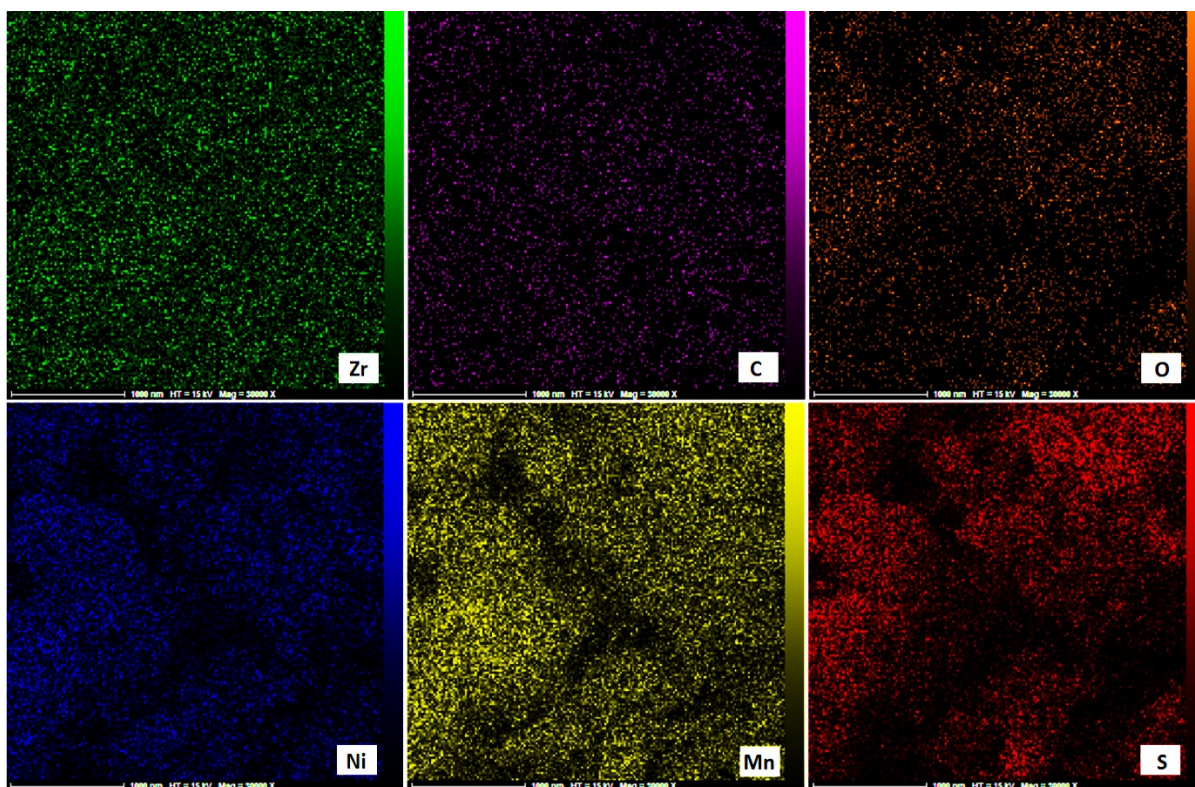


Figure S3. The elemental mapping of NU@LDHS composites.

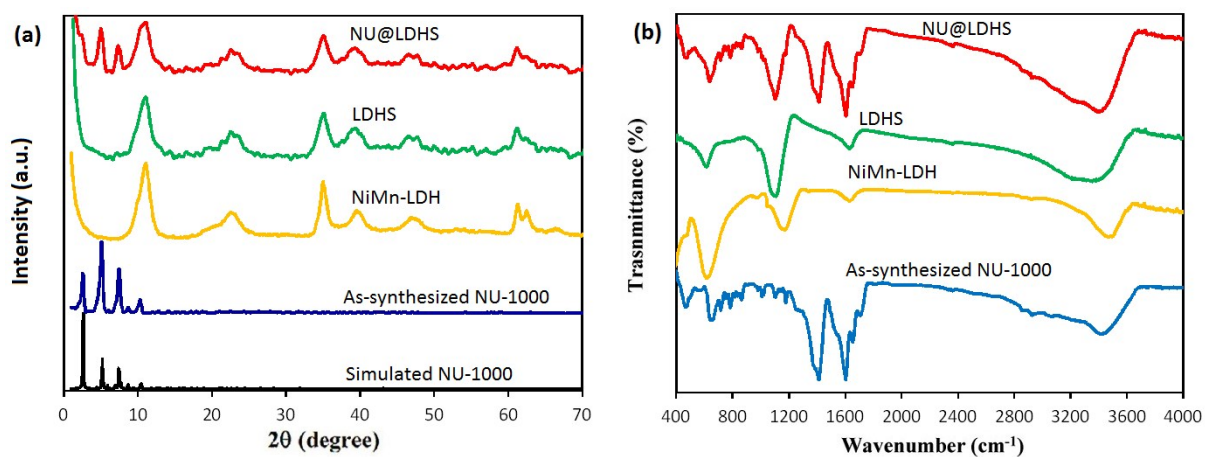


Figure S4. PXRD patterns (a) and FT-IR spectra (b) of as-synthesized NU, LDHS, and NU@LDHS composites.

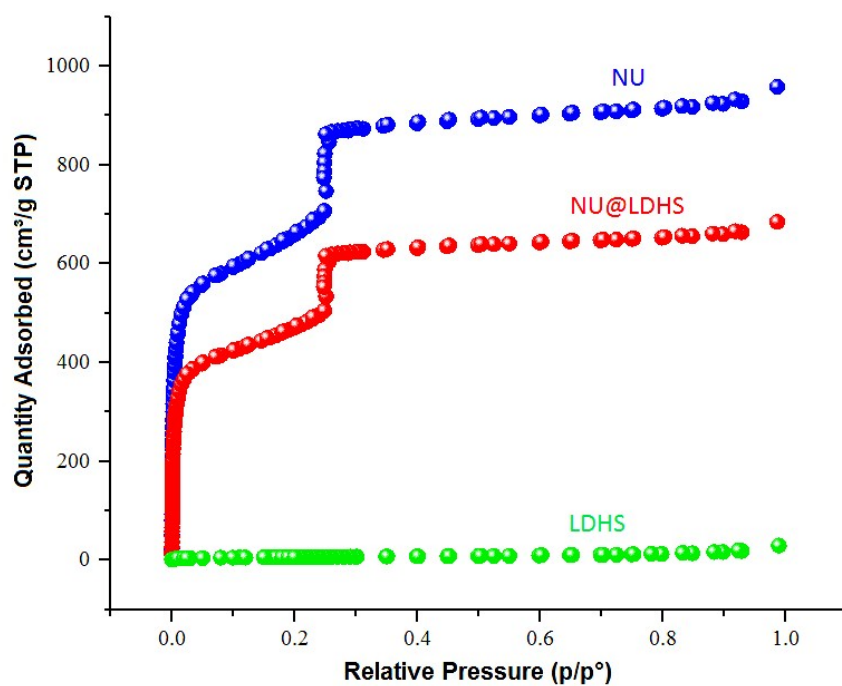


Figure S5. N₂ adsorption–desorption isotherms collected at 77 K for the as-synthesized NU, LDHS, and NU@LDHS composites.

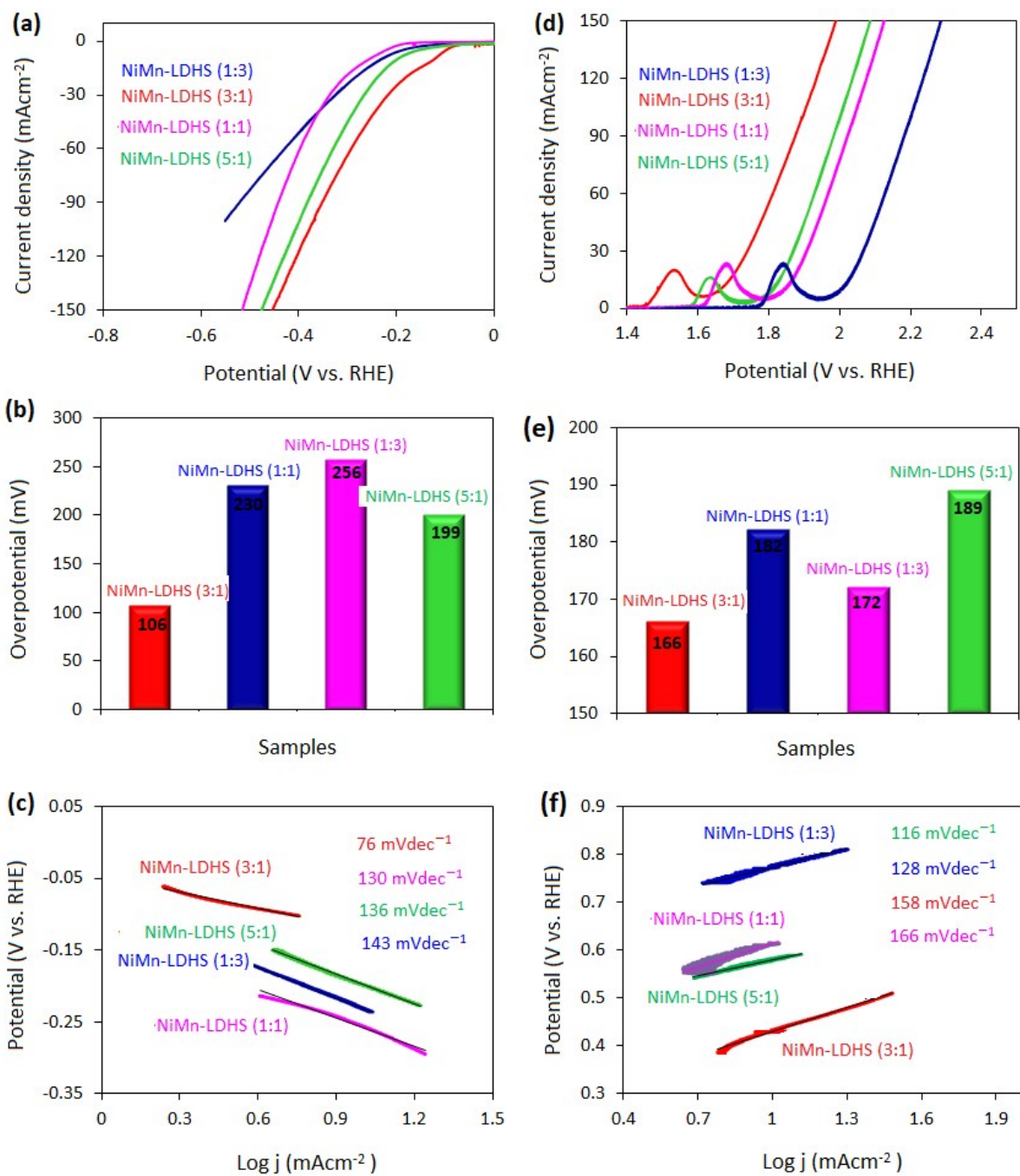


Figure S6. (a) LSV curves of NiMn-LDHS samples with different ratios for HER performance, (b) overpotentials for HER performance at 10 mAcm⁻² current densities, (c) Tafel plots derived from LSV curves, (d) LSV curves of NiMn-LDHS samples with different ratios for OER performance, (e) overpotentials for OER performance at 10 mAcm⁻² current densities and (f) Tafel plots derived from LSV curves.

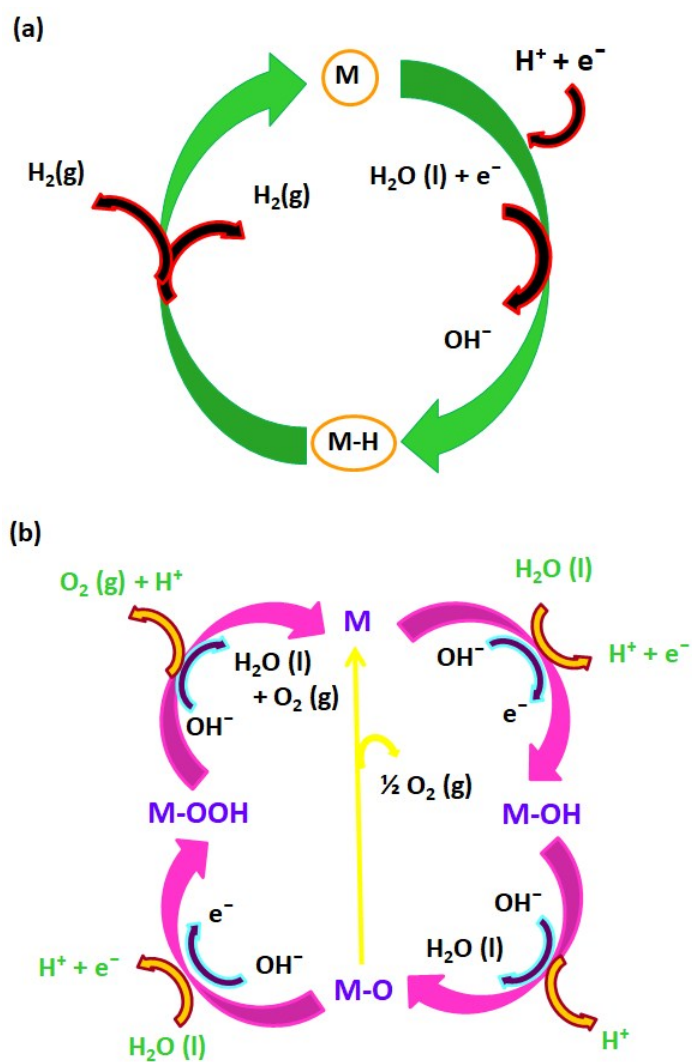


Figure S7. Schematic illustration of hydrogen generation (a) and oxygen generation (b) by electrochemical water splitting.

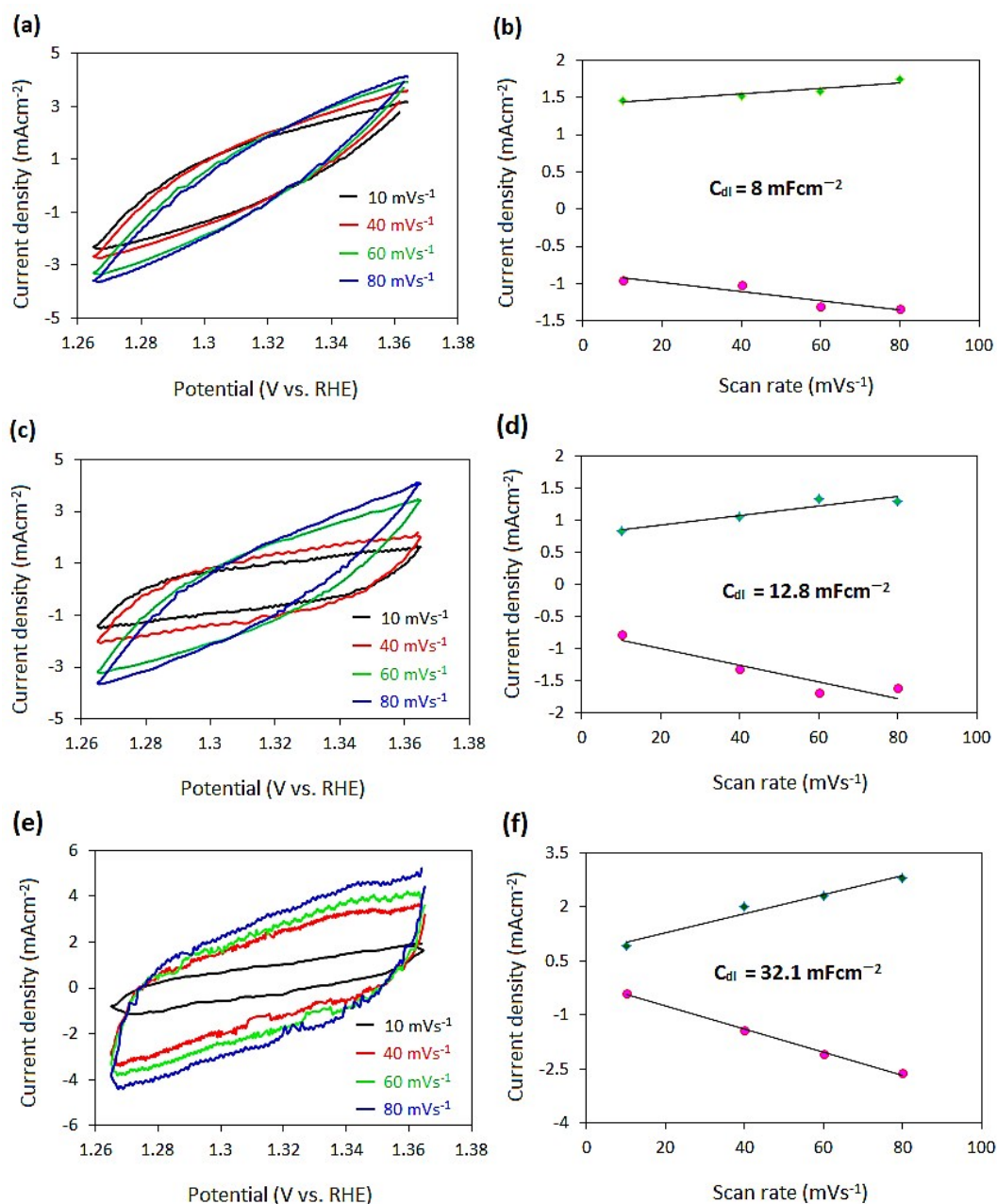


Figure S8. (a) CV curves of LDHS at different scan rates, (b) i-scan rates curves of LDHS electrocatalyst, (c) CV curves of NU electrocatalyst at different scan rates, (d) i-scan rates curves of NU electrocatalyst, (e) CV curves of NU@LDHS at different scan rates and (f) i-scan rates curves of NU@LDHS electrocatalyst.

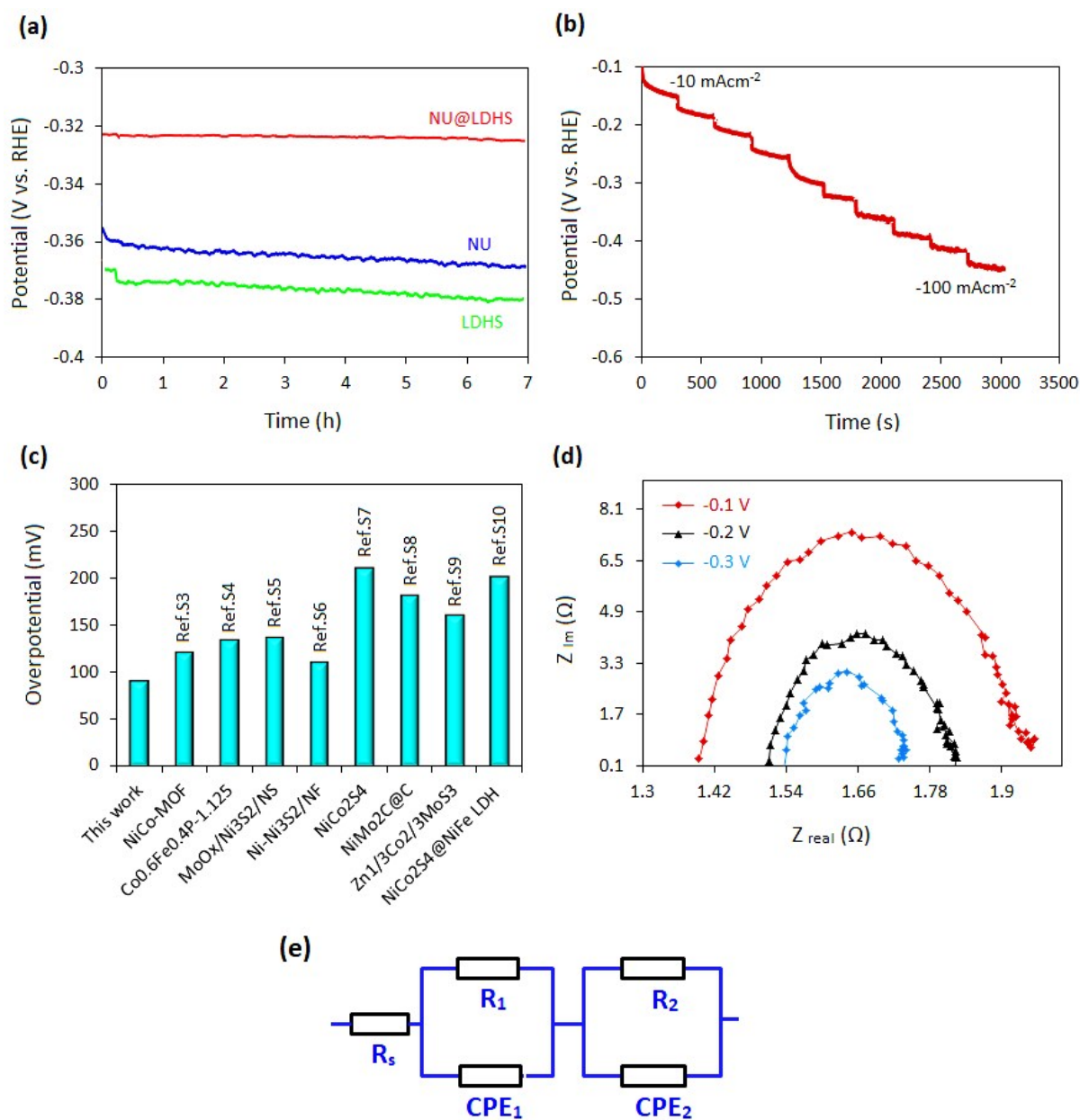


Figure S9. (a) Stability test of samples at 100 mA cm⁻² current density, (b) multistep chronopotentiometry curves for HER performance from 10 to 100 mA cm⁻² current densities, (c) comparison of overpotentials for HER performance at 10 mA cm⁻² current density with literature, (d) Nyquist plots of NU@LDHS at different overpotentials and (e) equivalent circuit used for EIS data.

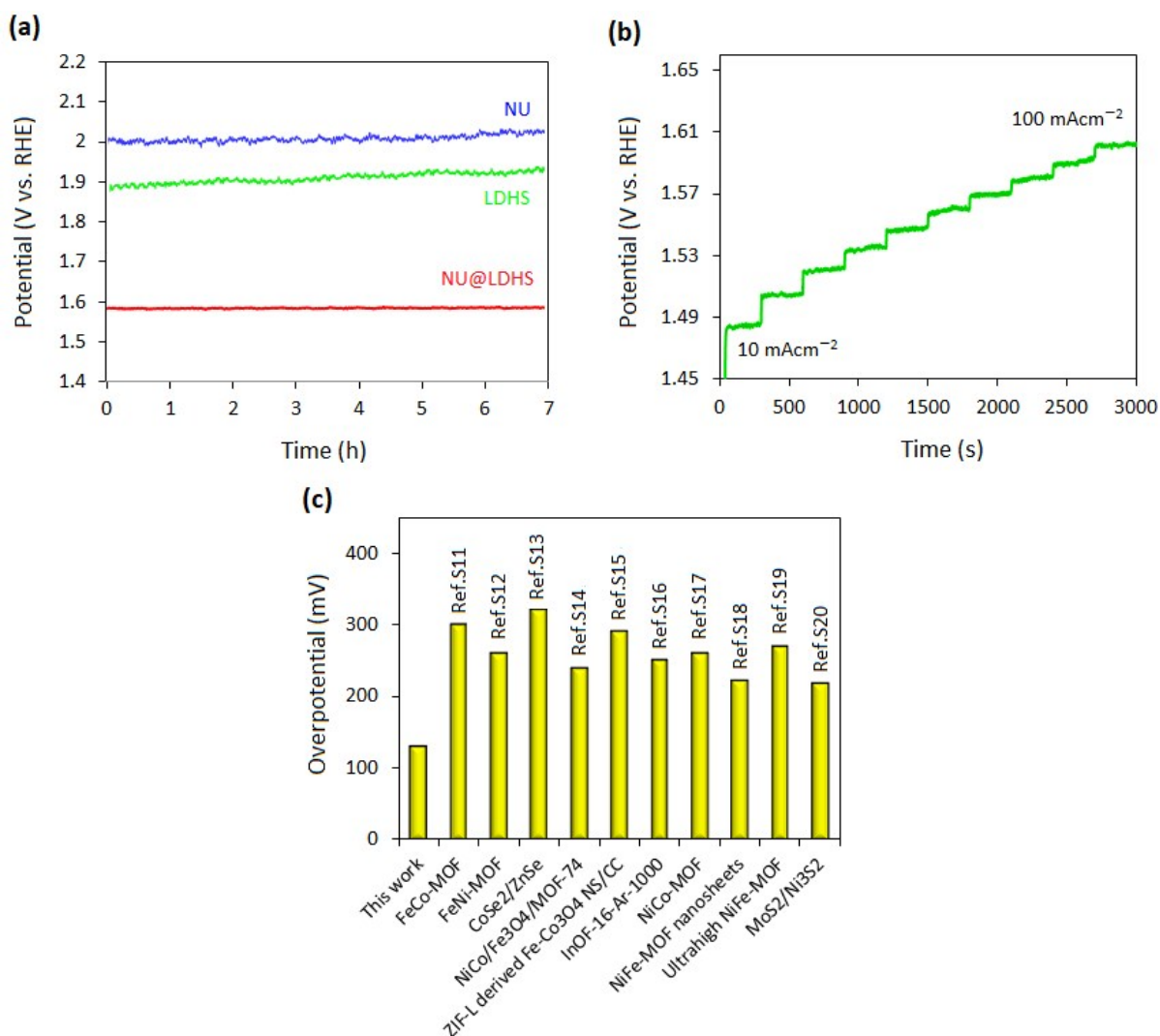


Figure S10. (a) Stability test of samples at 100 mA cm⁻² current density, (b) multistep chronopotentiometry curves from 10 to 100 mA cm⁻² and (c) comparison of overpotentials at 10 mA cm⁻² of present work with literature.

References

- S1 J. E. Mondloch, W. Bury, D. Fairen-Jimenez, S. Kwon, E. J. DeMarco, M. H. Weston, A. A. Sarjeant, S. T. Nguyen, P. C. Stair, R. Q. Snurr, O. K. Farha and J. T. Hupp, *J. Am. Chem. Soc.*, 2013, **135**, 10294–10297.
- S2 D. Feng, Z.-Y. Gu, J.-R. Li, H.-L. Jiang, Z. Wei and H.-C. Zhou, *Angew. Chem. Int. Ed.*, 2012, **51**, 10307–10310.
- S3 M. Liu, W. Zheng, S. Ran, S.T. Boles and L. Y. S. Lee, *Adv. Mater. Interfaces*, 2018, **21**, 1800849.
- S4 Y. Lian, H. Sun, X. Wang, P. Qi, Q. Mu, Y. Chen, J. Ye, X. Zhao, Z. Deng and Y. Peng, *Chem. Sci.*, 2019, **10**, 464–474.
- S5 Y. Wu, G. D. Li, Y. Liu, L. Yang, X. Lian, T. Asefa, and X. Zou, *Adv. Func. Mater.*, 2016, **26**, 4839-4847.
- S6 P. Chen, T. Zhou, M. Zhang, Y. Tong, C. Zhong, N. Zhang, L. Zhang, C. Wu and Y. Xie, *Adv. Mater.*, 2017, **29**, 1701584.
- S7 A. Sivanantham, P. Ganesan, and S. Shanmugam, *Adv. Func. Mater.*, 2016. **26**, 4661–4672.
- S8 X. Li, L. Yang, T. Su, X. Wang, C. Sun and Z. Su, *J. Mater. Chem. A*, 2017, **5**, 5000–5006.
- S9 L. Zhang, L. Yang, G. Xu, W. Wang, H. Song, C. Wang and D. Jia, *ACS Sustainable Chem. Eng.*, 2019, **7**, 9800–9807.
- S10 J. Liu, J. Wang, B. Zhang, Y. Ruan, L. Lv, X. Ji, K. Xu, L. Miao and J. Jiang, *ACS Appl. Mater. Interfaces*, 2017, **9**, 15364–15372.
- S11 J. Gao, J. Cong, Y. Wu, L. Sun, J. Yao and B. Chen, *ACS Appl. Energy Mater.*, 2018, **1**, 5140–5144.
- S12 J. Li, W. Huang, M. Wang, S. Xi, J. Meng, K. Zhao, J. Jin, W. Xu, Z. Wang, X. Liu, Q. Chen, L. Xu, X. Liao, Y. Jiang, K. A. Owusu, B. Jiang, C. Chen, D. Fan, L. Zhou and L. Mai, *ACS Energy Lett.*, 2019, **4**, 285–292.
- S13 G. Fang, Q. Wang, J. Zhou, Y. Lei, Z. Chen, Z. Wang, A. Pan and S. Liang, *ACS Nano*, 2019, **13**, 5635–5645.
- S14 X. Wang, H. Xiao, A. Li, Z. Li, S. Liu, Q. Zhang, Y. Gong, L. Zheng, Y. Zhu, C. Chen, D. Wang, Q. Peng, L. Gu, X. Han, J. Li and Y. Li, *J. Am. Chem. Soc.*, 2018, **140**, 15336–15341.

- S15 Y. Li, W. Zhu, X. Fu, Y. Zhang, Z. Wei, Y. Ma, T. Yue, J. Sun and J. Wang, *Inorg. Chem.*, 2019, **58**, 6231–6237.
- S16 J. Qian, T.-T. Li, Y. Hu and S. Huang, *Chem. Commun.*, 2017, **53**, 13027–13030.
- S17 D.-J. Li, Q.-H. Li, Z.-G. Gu and J. Zhang, *J. Mater. Chem. A*, 2019, **7**, 18519–18528.
- S18 R. L. Greenaway, V. Santolini, A. Pulido, M. A. Little, B. M. Alston, M. E. Briggs, G. M. Day, A. I. Cooper and K. E. Jelfs, *Angew. Chem. Int. Ed.*, 2019, **131**, 16421–16427.
- S19 X. Li, D.-D. Ma, C. Cao, R. Zou, Q. Xu, X.-T. Wu and Q.-L. Zhu, *Small*, 2018, **15**, 1902218.
- S20 J. Zhang, T. Wang, D. Pohl, B. Rellinghaus, R. Dong, S. Liu, X. Zhuang and X. Feng, *Angew. Chem.*, 2016, **55**, 6702–6707.